



AMS

American Meteorological Society

Supplemental Material

Journal of Climate

Two Approaches of the Spring North Atlantic Sea Surface Temperature Affecting the
Following July Precipitation over Central China: The Tropical and Extratropical
Pathways

<https://doi.org/10.1175/JCLI-D-21-1012.1>

© Copyright 2022 American Meteorological Society (AMS)

For permission to reuse any portion of this work, please contact permissions@ametsoc.org. Any use of material in this work that is determined to be “fair use” under Section 107 of the U.S. Copyright Act (17 USC §107) or that satisfies the conditions specified in Section 108 of the U.S. Copyright Act (17 USC §108) does not require AMS’s permission. Republication, systematic reproduction, posting in electronic form, such as on a website or in a searchable database, or other uses of this material, except as exempted by the above statement, requires written permission or a license from AMS. All AMS journals and monograph publications are registered with the Copyright Clearance Center (<https://www.copyright.com>). Additional details are provided in the AMS Copyright Policy statement, available on the AMS website (<https://www.ametsoc.org/PUBSCopyrightPolicy>).

Table S1. A list of 15 CMIP6/AMIP models used in this study.

Model name	Institution
ACCESS-CM2	Commonwealth Scientific and Industrial Research Organisation, and Australian Research Council Centre of Excellence for Climate System Science, Australia
ACCESS-ESM1-5	
BCC-CSM2-MR	Beijing Climate Center, China
BCC-ESM1	
CAMS-CSM1-0	Chinese Academy of Meteorological Sciences, China
CanESM5	Canadian Centre for Climate Modelling and Analysis, Canada
CESM2	National Center for Atmospheric Research, USA
CESM2-FV2	
CESM2-WACCM	
CESM2-WACCM-FV2	
CNRM-CM6-1	Centre National de Recherches Météorologiques-Centre
CNRM-CM6-1-HR	Européen de Recherche et de Formation Avancée en
CNRM-ESM2-1	Calcul Scientifique, France
EC-Earth3	EC-Earth Consortium, Europe
EC-Earth3-Veg	

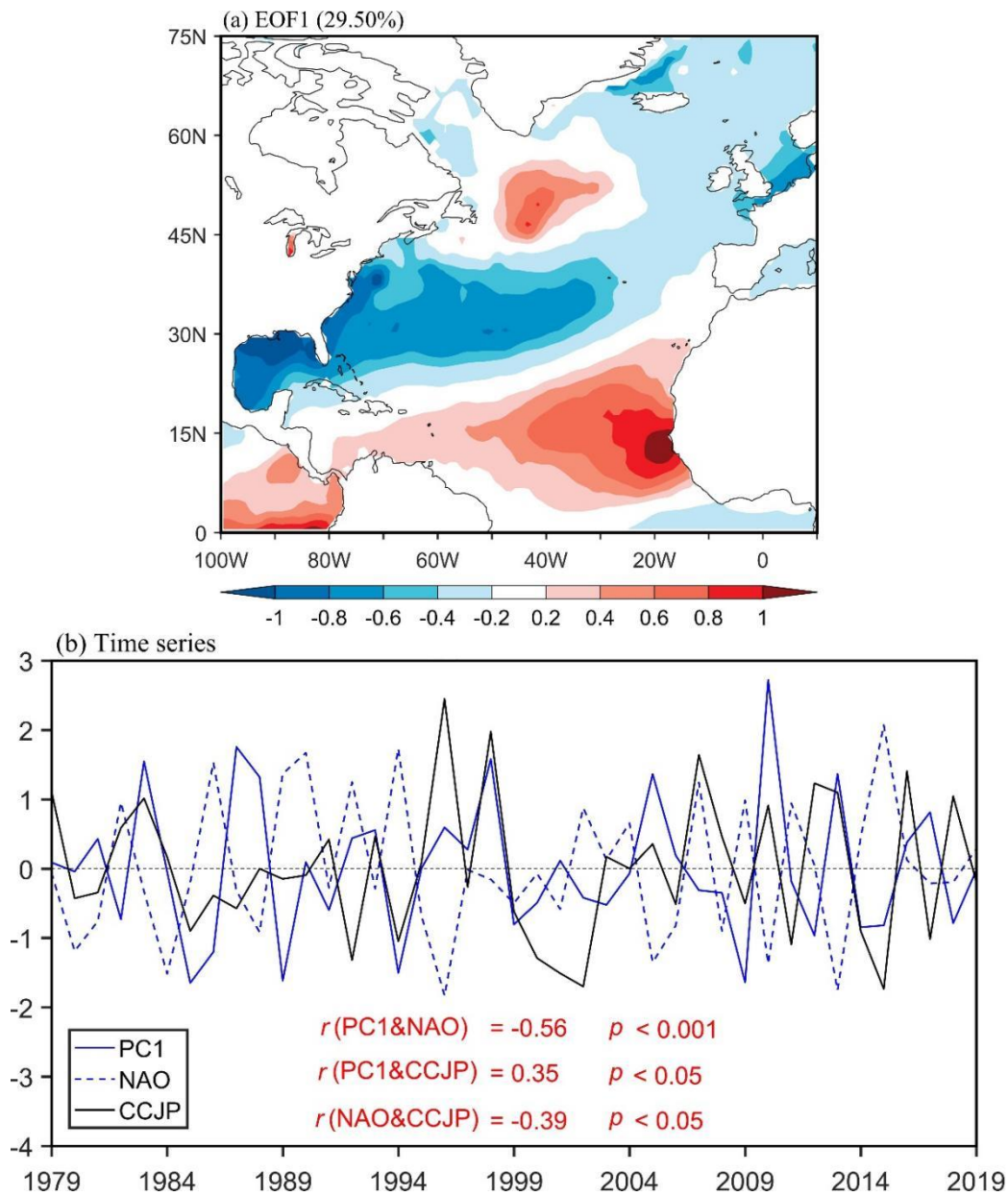


Figure S1. (a) The leading Empirical Orthogonal Function (EOF1) mode of spring SST ($^{\circ}\text{C}$) anomalies in North Atlantic during the period of 1979-2019. (b) Time series of the first principal component (PC1), the spring North Atlantic Oscillation (NAO) index and the CCJP index. The percentage at the top of (a) indicates the variance explained by the EOF1 mode. $r(\text{PC1\&NAO})$, $r(\text{PC1\&CCJP})$ and $r(\text{NAO\&CCJP})$ in (b) are the correlation coefficients among the PC1, the spring NAO index and the CCJP index. All data are linearly detrended and standardized.

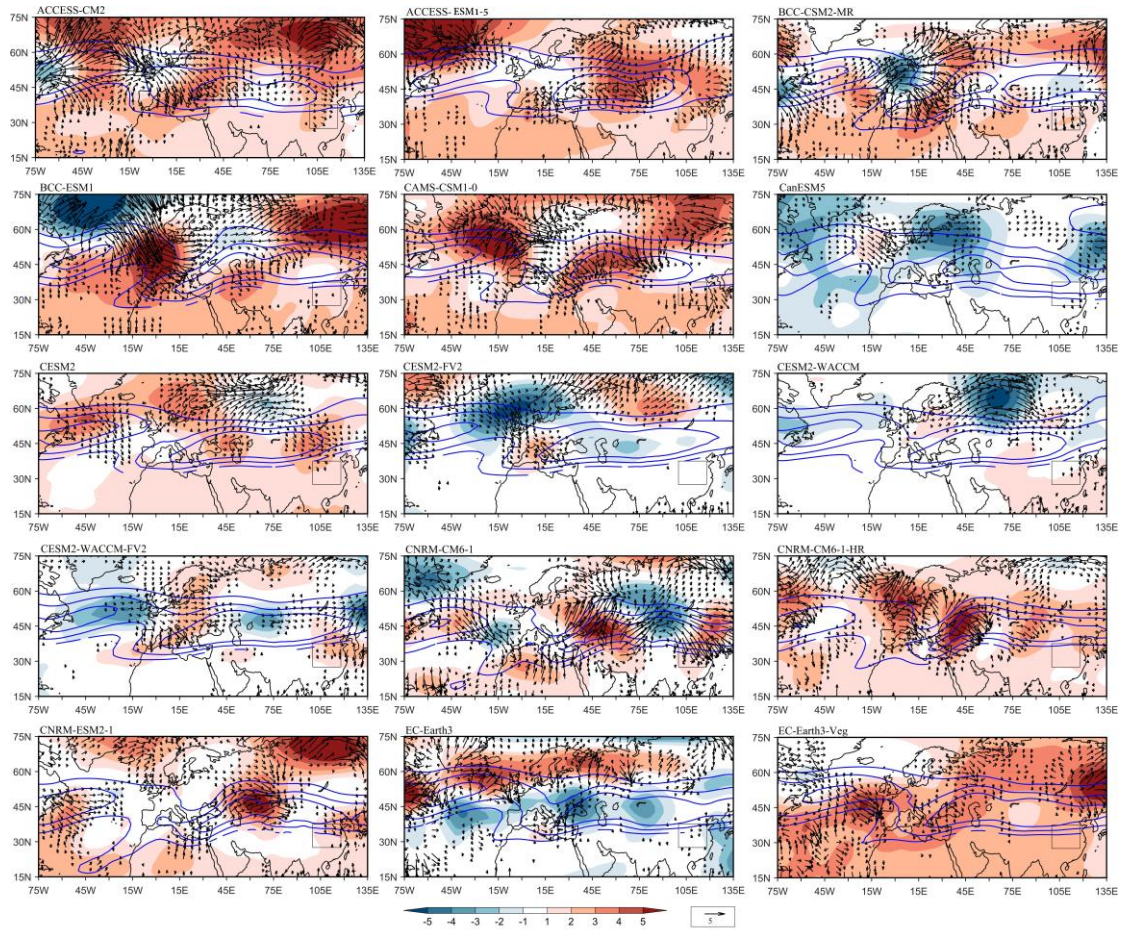


Figure S2. Regression map of the July 200-hPa streamfunction (shaded; $5 \times 10^5 \text{ m}^2 \text{ s}^{-1}$) and wave activity flux anomalies (arrows; $\text{m}^2 \text{ s}^{-2}$) onto the spring TSNA SST index in 15 CMIP6/AMIP models. The name of each model is given at the top of each figure. The blue solid lines are the 200-hPa zonal wind larger than 12 m s^{-1} , with intervals of 4 m s^{-1} , denoting the jet stream. Vector speeds less than $1 \text{ m}^2 \text{ s}^{-2}$ are not shown. The boxed area denotes the region of central China.

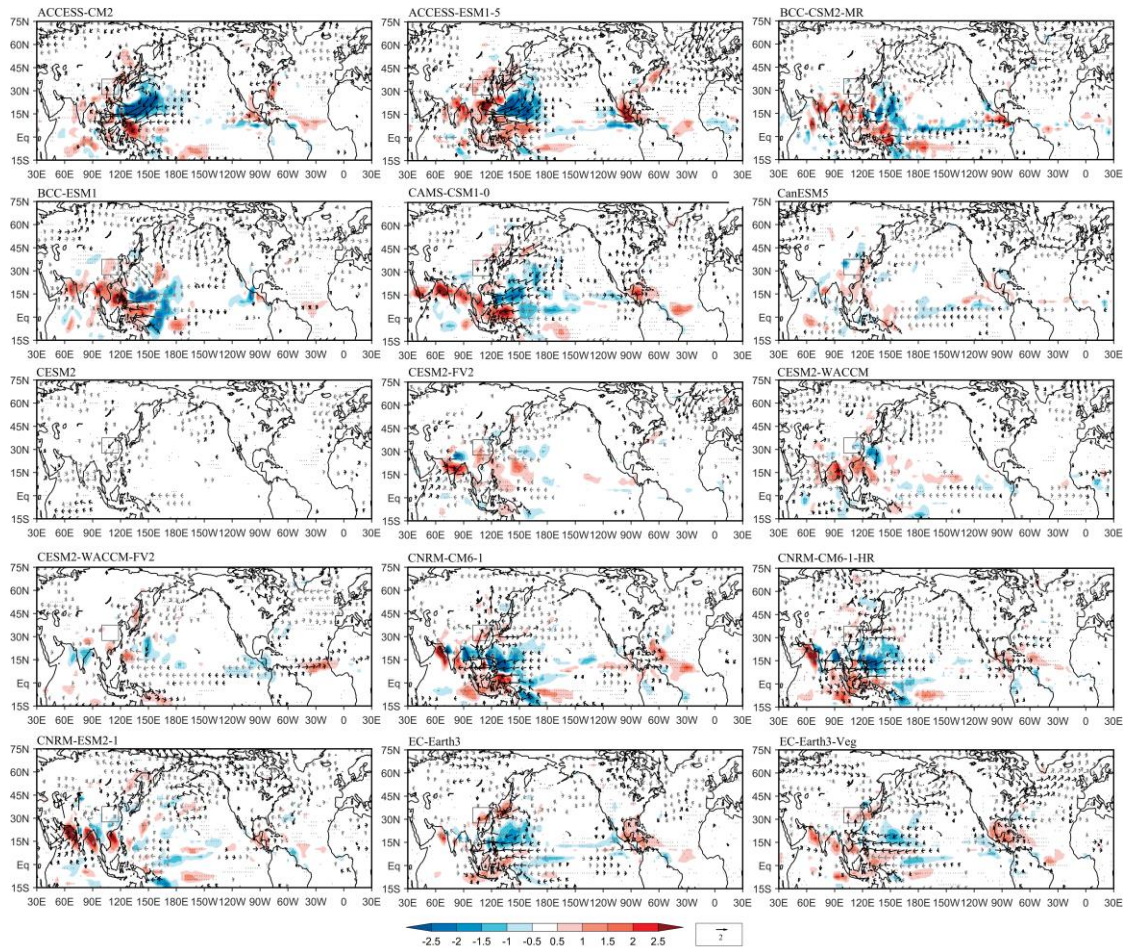


Figure S3. Regression map of the July precipitation anomalies (shaded; mm day^{-1}) and 850-hPa wind anomalies (vectors; m s^{-1}) onto the spring TSNA SST index in 15 CMIP6/AMIP models. The name of each model is given at the top of each figure. The dots indicate that the regressed precipitation anomalies are at the significance level of $p < 0.1$. The black arrows indicate that the zonal or meridional component of the wind anomalies exceed the significance level of $p < 0.1$. Wind speeds less than 0.5 m s^{-1} are not shown. The boxed area denotes the region of central China.